



HAL
open science

A method for predicting the reverberation time and decay curves of rectangular rooms with non-uniform absorption distribution using Statistical Energy Analysis

Laurence Wilmshurst, David Thompson

► To cite this version:

Laurence Wilmshurst, David Thompson. A method for predicting the reverberation time and decay curves of rectangular rooms with non-uniform absorption distribution using Statistical Energy Analysis. Acoustics 2012, Apr 2012, Nantes, France. hal-00810686

HAL Id: hal-00810686

<https://hal.science/hal-00810686>

Submitted on 23 Apr 2012

HAL is a multi-disciplinary open access archive for the deposit and dissemination of scientific research documents, whether they are published or not. The documents may come from teaching and research institutions in France or abroad, or from public or private research centers.

L'archive ouverte pluridisciplinaire **HAL**, est destinée au dépôt et à la diffusion de documents scientifiques de niveau recherche, publiés ou non, émanant des établissements d'enseignement et de recherche français ou étrangers, des laboratoires publics ou privés.



ACOUSTICS 2012

A method for predicting the reverberation time and decay curves of rectangular rooms with non-uniform absorption distribution using Statistical Energy Analysis

L. I. Wilmshurst and D. J. Thompson

Dynamics Group-ISVR - University of Southampton, University Road, SO17 1BJ
Southampton, UK
lwilmshurst@hotmail.co.uk

The subject of reverberation time in non-diffuse environments has been of considerable interest since the inception of room acoustics in the early twentieth century. Various prediction methods have been developed with the aim of accurately predicting the reverberation time of an enclosure under these circumstances; a completely universal method has yet to be devised. This paper examines the decay processes in rooms where absorption is unevenly distributed, which is a common occurrence in practice and often leads to a non-diffuse sound field. In order to establish the nature of these decay processes, a seven-subsystem Statistical Energy Analysis model has been developed, based initially on the axial, tangential and oblique mode groups and then extended to include the dimensions of formation. The damping and coupling loss factors are established analytically from the absorption and scattering coefficients of the walls respectively. For homogeneous (evenly distributed absorption) rooms, the relative diffusivity is established using the absorption and scattering parameters. For non-homogeneous enclosures, the validity of the results obtained using this method is tested using various computer simulations.

1 Introduction

In 1959, Fitzroy [1] published a paper highlighting the fallibility of the Sabine formula as a method for predicting the reverberation time of rooms with a non-uniform absorption distribution. One prominent example featured a ceiling with all-over acoustical treatment, leaving the floor and walls relatively untreated. Here, it was shown that the Sabine formula predicted reverberation times that were far shorter in duration than the measured reverberation times.

These inaccuracies have serious implications in the realm of building acoustics; new structures in the UK typically have to comply with regulations set out in Approved Document E [2] and Building Bulletin 93 [3], and imprecise predictions may result in the regulations not being met or excessive treatment being applied.

Unfortunately, rooms with uneven absorption distributions are more common in practice than ideal 'Sabine' rooms, and so a variety of methods have been devised for the purpose of overcoming this problem, ranging from modified prediction formulae [1, 4-6] to ray-tracing computer software such as CATT-Acoustic [7] and ODEON [8].

Nilsson [9] studied the absorbing ceiling scenario extensively, and postulated a method for this particular case. The method is based on Statistical Energy Analysis (SEA), a high-frequency energy transmission model used for predicting the transmission of sound in complex structures with many resonant modes [10]. Here, the sound field is sub-divided into two components, comprising grazing modes and non-grazing modes (where the latter are at oblique incidence to the ceiling), for calculating the reverberation time.

This work aims to extend such an SEA model to accommodate arbitrary absorption distributions, which can be achieved by sub-dividing the sound field into the axial, tangential, and oblique mode groups, and then sub-dividing further by accounting for the possible direction(s) of the mode groups (shown in Figure 1). The result is a seven-subsystem SEA model.

2 Energy Decay Modelling

There are several advantages offered through using SEA for predicting reverberation times. One of the most crucial benefits is that the SEA model calculates the total acoustic potential energy in the enclosure as a function of time, and so a theoretical energy decay curve is obtained. This gives far more insight into the acoustic characteristics of the rooms than a prediction formula would reveal, particularly in regards to the decay processes. In particular, an enclosure

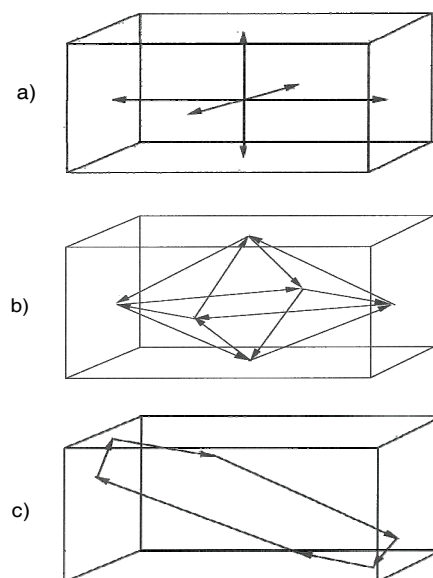


Figure 1: Possible directions associated with a) axial modes b) tangential modes c) oblique modes.

with a sound field that is approximately diffuse will exhibit an almost linear decay curve. Conversely, the decay curves of rooms with non-diffuse sound fields are typically non-linear due to the presence of multiple decay rates that depend on the direction of the sound waves. In the SEA model, the energy decay rates are primarily determined by the damping loss factors η_d and the coupling loss factors η_c , and so the relative 'diffusivity' of the modelled enclosure can be directly attributed to these parameters.

It is also possible to relate the damping loss factors and coupling loss factors of the modelled enclosure to the absorption and scattering coefficients of each surface respectively. The latter offers an advantage to the experimental approach suggested by Nilsson [9] in terms of simplicity, given that no additional measurements are required. Furthermore, these definitions allow various SEA phenomena to be explained easily in physical terms; for instance, if the Smith criterion for strong coupling [10] is satisfied ($\eta_c \ll \eta_d$), the law of equipartition applies, where the modal energies are equal and the coupling loss factors become irrelevant. In this case, the decay curve is linear, and the sound field in the enclosure is therefore diffuse.

Additional parameters for the SEA model include the mode counts and initial energies of each subsystem. Analytical expressions for these variables can be derived fairly easily using the wave-theoretical analysis presented by Morse and Bolt [11] in the 1940's, and are illustrated in the next section alongside the loss factors.

It is standard procedure to express the reverberation time of an enclosure in terms of octave or one-third octave frequency bands. The SEA model utilises the octave bands by expressing the various parameters according to the angular frequency limits $\omega_{lower,upper}$ and centre frequency ω_c of the octave band in question.

3 Theory

3.1 SEA Modelling

By assuming that the system has reached a steady-state and the source is turned off, the vector of energies $\{\mathbf{E}(t)\}$ will decay from its initial values $\{\mathbf{E}(0)\}$. In this case, the decay processes can be modelled by a series of coupled equations:

$$\frac{d}{dt}\{\mathbf{E}(t)\} + \omega_c \mathbf{L}\{\mathbf{E}(t)\} = 0 \quad t \geq 0 \quad (1)$$

where \mathbf{L} is the 7 x 7 loss factor matrix that contains the damping loss factors η_i and coupling loss factors η_{ij} :

$$\mathbf{L} = \begin{bmatrix} \eta_1 + \xi_1 & -\eta_{21} & \cdots & -\eta_{71} \\ -\eta_{12} & \eta_2 + \xi_2 & \cdots & -\eta_{72} \\ \vdots & \vdots & \ddots & \vdots \\ -\eta_{17} & -\eta_{27} & \cdots & \eta_7 + \xi_7 \end{bmatrix}. \quad (2)$$

Here, the parameter ξ_i is determined using:

$$\xi_i = \sum_{i \neq j}^N \eta_{ij}. \quad (3)$$

where i and j denote the transmission and recipient subsystems respectively. Information on the mode groups and relevant dimension(s) for each subsystem is shown in Table 1.

Table 1: Details of SEA subsystems.

Subsystem	Mode Groups	Direction(s)
1	Axial	x
2	Axial	y
3	Axial	z
4	Tangential	xy
5	Tangential	xz
6	Tangential	yz
7	Oblique	-

The decay constants of the uncoupled subsystems are found from the eigenvalues Λ of the loss factor matrix, and the uncoupled energies are obtained from the eigenvector matrix Φ . Taking the Laplace transform of Eq. (1) and pre-multiplying by Φ then yields the general solution to Eq. (1):

$$\{\mathbf{E}(t)\} = \text{diag}(\Phi\{\mathbf{E}(0)\})\{e^{-\omega_c \Lambda t}\} \quad (4)$$

However, it should be noted that the eigenvector components in Φ are typically subject to arbitrary scaling, which is undesirable. The eigenvector matrix Φ can be rescaled appropriately to Φ_S such that the contributions of each of the eigenvector components are the same, and is achieved using:

$$\Phi_S = \{\gamma\}\Phi, \quad \{\gamma\} = (\{\mathbf{E}(0)\}\mathbf{I})^{-1}\Phi^{-1}\{\mathbf{E}(0)\}. \quad (5,6)$$

Once the modified eigenvector matrix Φ_S is substituted into Φ , the total energy in the enclosure as a function of time can be established by applying Eq. (4), and then summing the energy vector $\{\mathbf{E}(t)\}$ for each time block. The derivations of each parameter in Eq. (4) are explained in the next section.

3.2 SEA Parameters

Since Λ and Φ can be obtained from the loss factor matrix, the primary unknown in Eq. (4) is the vector of initial energies $\{\mathbf{E}(0)\}$. This parameter is ascertained using the 7 x 1 *energy-per-mode* vector $\{\mathbf{E}_{mode}\}$ and the 7 x 1 mode count vector, denoted as $\{\mathbf{N}_{mode}\}$:

$$\{\mathbf{E}(0)\} = \text{diag}(\mathbf{E}_{mode})\{\mathbf{N}_{mode}\}$$

$$\{\mathbf{N}_{mode}\} = [N_{ax} \ N_{ax} \ N_{ax} \ N_{tan} \ N_{tan} \ N_{tan} \ N_{ob}]^T \quad (7,8)$$

where N_{ax} , N_{tan} and N_{ob} are the mode counts of each subsystem in Table 1. The expressions for Eq. (8) are obtained from Kuttruff's eigenfrequency lattice [12]:

$$\begin{aligned} N_{ax} &= \frac{(k_{upper} - k_{lower})L_{x,y,z}}{\pi} \\ N_{tan} &= \frac{L_{x,y,z}L_{x,y,z}(k_{upper}^2 - k_{lower}^2)}{4\pi} - \frac{(N_{ax,i} + N_{ax,j})}{2} \\ N_{ob} &= \frac{V(k_{upper}^3 - k_{lower}^3)}{6\pi^2} - \frac{N_{tan,tot}}{2} - \frac{N_{ax,tot}}{4} \\ N_{tan,tot} &= (N_{tan,ij} + N_{tan,il} + N_{tan,jl}) \\ N_{ax,tot} &= (N_{ax,i} + N_{ax,j} + N_{ax,l}) \end{aligned} \quad (9)$$

where l is an additional subsystem subscript, $L_{x,y,z}$ is the room dimension in the direction of the relevant subscript, V is the room volume, and k_{upper} and k_{lower} are the upper and lower limits of the octave band respectively, in terms of the acoustic wavenumber k .

The decay processes of the enclosure are determined by the *relative* energy levels of the subsystems, and it is therefore reasonable to normalise $\{\mathbf{E}_{mode}\}$ such that the energy-per-mode of the oblique mode group is unity. It is shown by Morse and Bolt [11] that if the mode shapes are normalised, an axial mode has approximately four times more energy than an oblique mode, and a tangential mode has twice the energy of an oblique mode. Therefore:

$$\{\mathbf{E}_{mode}\} = [4 \ 4 \ 4 \ 2 \ 2 \ 2 \ 1]^T \quad (10)$$

The damping loss factors of the subsystems were calculated using three different methods for the purposes of analysis and comparison [13], where the most appropriate method was chosen for each case. First, the damping loss factors for each individual surface were ascertained according to the incidence of the waves that form the subsystem in question to the surface (i.e. normal-incidence, two-dimensional random-incidence, three-dimensional random-incidence, and grazing-incidence). The total damping loss factors were then obtained by summing the individual damping loss factors for each surface accordingly.

The normal-incidence damping loss factor $\eta_{norm,i}$ is found from the normal-incidence absorption coefficient α_n :

$$\eta_{norm,W} = \frac{\cos^{-1}\left(\frac{(\sigma - \mu)(1 + R_n^2)}{2R_n(\sigma + \mu)}\right)}{L_{x,y,z}k_c}, \quad \sigma = 1 + R_n^2 + 2R_n,$$

$$\mu = 2(1 + R_n^2 - 2R_n), \quad R_n = \sqrt{1 - \alpha_n^2} \quad (11,12,13,14)$$

where n is the surface subscript, R_n is the reflection coefficient of the surface, and k_c is the centre frequency of the octave band in terms of the acoustic wavenumber. In order to apply Eq. (14), it is assumed that R_n is real, which holds provided the surface is sufficiently rigid.

The expressions for the two-dimensional (tangential) and three-dimensional (oblique) random-incidence damping loss factors ($\eta_{2D,n}$ and $\eta_{3D,n}$ respectively) are:

$$\eta_{2D,n} = -\frac{c_0 \ln(1 - \alpha_{r,n})}{\pi \omega_c L_{x,y,z}}, \quad \eta_{3D,n} = -\frac{S c_0 \ln(1 - \alpha_{r,n})}{4 \omega_c V} \quad (15,16)$$

where c_0 is the speed of sound in air and $\alpha_{r,n}$ is the random-incidence absorption coefficient of the surface. It should be noted that Eq. (16) only holds if the sound field is diffuse; for the non-diffuse case, Eq. (16) reverts to:

$$\eta_{3D,n} = -\frac{2c_0 \ln(1 - \alpha_{r,n})}{\pi^2 \omega_c L_{x,y,z}} \quad (17)$$

The grazing-incidence loss factor was obtained using a method shown by Nilsson [9] for a pressure-release surface:

$$\eta_{graz,n} = \frac{\pi^2}{2} \left[\zeta_n \left(\frac{1}{k_c L_{x,y,z}} \right)^3 \right] \quad (18)$$

where ζ_n is the non-dimensional acoustic impedance of the surface, which is assumed to be real. This enables the total damping loss factors for each type of subsystem (η_{ax} , η_{tan} , η_{ob}) to be calculated using:

$$\eta_{ax} = \sum_{s=1}^2 \eta_{norm,n} + \sum_{s=1}^4 \eta_{graz,n}, \quad \eta_{tan} = \sum_{s=1}^4 \eta_{2D,n} + \sum_{s=1}^2 \eta_{graz,n}, \quad \eta_{ob} = \sum_{s=1}^6 \eta_{3D,n} \quad (19)$$

These damping loss factors are shown as a function of the average absorption coefficient for a homogeneous 5 x 4 x 3 metre enclosure in Figure 2 as an example.

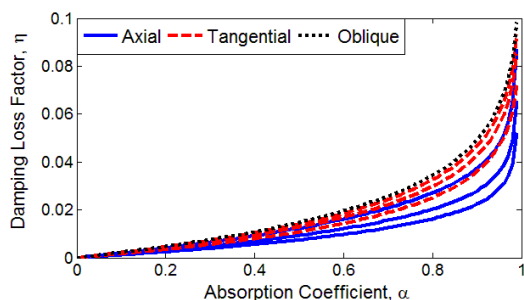


Figure 2: The damping loss factors as a function of the absorption coefficient. The centre frequency of the octave band is 1 kHz, and it is assumed that the sound field is diffuse.

The coupling loss factors were obtained using the power transmission W_{ij} between the subsystems i and j , which is ascertained from the random-incidence scattering coefficient s by assuming a Lambertian scattering surface. The following equation is then applied:

$$\eta_{ij} = \frac{W_{ij}}{\omega_c E_i} \quad (20)$$

The expressions for the coupling loss factors of an individual surface are:

$$\eta_{ax,ax,n} = 0, \quad \eta_{ax,tan,n} = \eta_{tan,ob,n} = \frac{8c_0 S_n N_j s (1 - \alpha_{r,n})}{\pi \omega_c V N_{hem}},$$

$$\eta_{ax,ob,n} = \frac{2c_0 S_n N_j s (1 - \alpha_{r,n})}{\pi \omega_c V N_{hem}},$$

$$\eta_{tan,tan,n} = \frac{32c_0 S_n N_j s (1 - \alpha_{r,n})}{\pi^2 \omega_c V N_{hem}}$$

$$N_{hem} = 4N_{ob} + 2N_{tan,tot} + N_{ax,tot} \quad (21)$$

where S_n is the area of the surface, N_{hem} is four times the total number of modes in the enclosure within the octave band and N_j is the number of modes in the recipient subsystem. It is possible to swap the initial and recipient subsystems by simply altering N_j for the new recipient subsystem. The total coupling loss factors are then obtained by summing the contributions of each of the common surfaces shared by the two subsystems:

$$\eta_{ax,i} = \sum_{n=1}^2 \bar{\eta}_{ax,i,n}, \quad \eta_{tan,ax} = \sum_{n=1}^2 \bar{\eta}_{tan,ax,n},$$

$$\eta_{tan,tan} = \sum_{n=1}^2 \eta_{tan,tan,n}, \quad \eta_{tan,ob} = \sum_{n=1}^4 \eta_{tan,ob,n},$$

$$\eta_{ob,ax} = \sum_{n=1}^2 \eta_{ob,ax,n}, \quad \eta_{ob,tan} = \sum_{n=1}^4 \eta_{ob,tan,n} \quad (22)$$

where

$$\bar{\eta}_{ax,i,n} = \begin{cases} \eta_{ax,i,n} & \text{if common surfaces exist} \\ 0 & \text{if no common surfaces exist.} \end{cases} \quad (23)$$

$$\bar{\eta}_{tan,ax,n} = \begin{cases} \eta_{tan,ax,n} & \text{if common surfaces exist} \\ 0 & \text{if no common surfaces exist.} \end{cases} \quad (24)$$

The total coupling loss factors are shown as a function of the scattering coefficient for the 5 x 4 x 3 metre enclosure in Figure 3. The centre frequency is 1 kHz and α_r is 0.05.

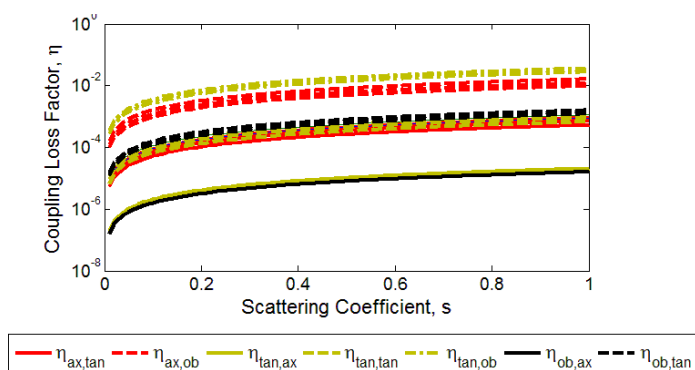


Figure 3: The coupling loss factors as a function of the scattering coefficient.

From Figure 3, it is evident that coupling is strongest into the oblique mode group and weakest into the axial mode groups. Therefore, if the scattering coefficient is sufficiently high, the subsystem energies will couple into the oblique mode group, which will thus dominate the decay process and result in an approximately diffuse field. The converse is true if the scattering coefficient is small.

4 Simulations

4.1 Homogeneous Enclosures

The reverberation time of a homogeneous 5 x 4 x 3 metre enclosure obtained using the SEA model is shown as a function of the average scattering coefficient in Figure 4.

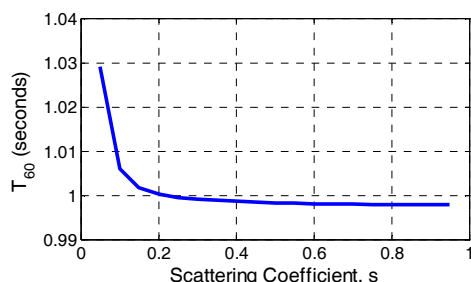


Figure 4: Reverberation time T_{60} at 1 kHz ($\alpha_r = 0.1$). It is evident that T_{60} tends to a limiting value as s is increased.

Once the scattering coefficient is high enough for the reverberation time to remain constant, the Smith criterion for strong coupling is satisfied, and the decay curve is linear, corresponding to a diffuse field. Therefore, the diffusive state of a homogenous enclosure can be established from the average absorption and scattering coefficients by calculating the *normalised gradient* $J(\alpha_r, s)$ of the reverberation time curve, as shown in Figure 4. This parameter is ascertained from the following expression:

$$J(\alpha_r, s) = \frac{\partial T_{60}}{\partial s} / T_{60}(\alpha_r, 0) \quad (25)$$

The resulting ‘diffusivity indicators’ are obtained for the enclosure shown in Figure 4, and are illustrated for the 500 Hz and 2 kHz octave bands in Figure 5.

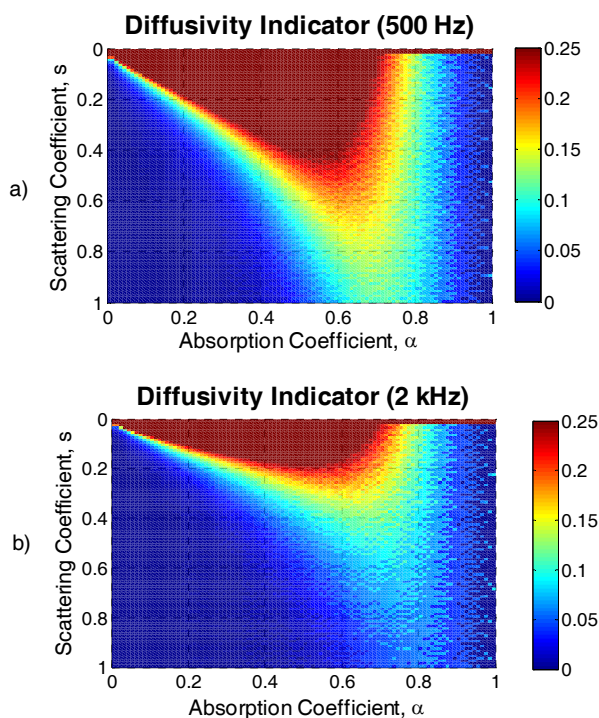


Figure 5: Variation of $J(\alpha_r, s)$ with the average absorption and scattering coefficient at a) 500 Hz and b) 2 kHz. The dark red and blue regions on the left of the figures ($\alpha_r < 0.8$) indicate large and small reverberation time gradients respectively.

In this case, the sound field is diffuse for values of $J(\alpha_r, s)$ lower than 0.05 – 0.1. From Figure 5, it is evident that there are fewer combinations of absorption and scattering coefficient that result in a diffuse field at 500 Hz than for 2 kHz, thereby confirming that the sound field is more likely to be diffuse at high frequencies.

In addition, Figure 5 shows that the sound field is diffuse for a large range of scattering coefficient values if the absorption coefficient is small ($\alpha_r < 0.1$). However, the possible combinations for a diffuse field become increasingly restricted to larger scattering coefficient values as the absorption coefficient is increased, which highlights that the sound field is less diffuse when the average absorption coefficient is large.

The reverberation time of the enclosure is also ascertained as a function of the average absorption coefficient α_r using the SEA model. The T_{60} values are compared with results obtained with the Sabine, Eyring [14] and EN 12354-6 [6] prediction formulae in Figure 6.

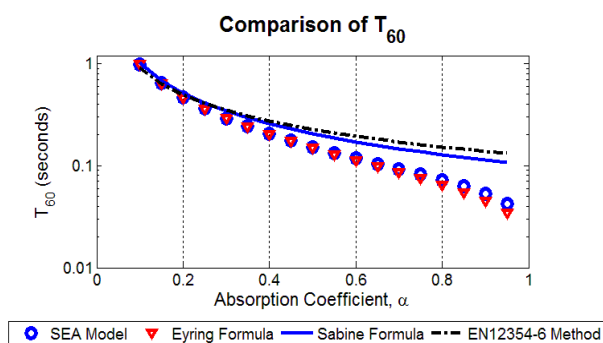


Figure 6: Reverberation times at 2 kHz obtained using the SEA model ($s = 0.5$) and various prediction methods.

Figure 6 shows that the SEA model agrees well with Eyring’s formula until $\alpha_r \approx 0.5$, where the SEA model gives longer predictions. In Figure 5b), the point $s = 0.5, \alpha_r = 0.5$ lies on the boundary between diffuse and non-diffuse behaviour, and so the deviation can be explained by the decreasing diffusivity of the sound field. Thus, the diffusivity indicators can be used to verify the validity of the diffuse field assumption used by the Sabine and Eyring formulae before predictions are made.

4.2 Non-Homogeneous Enclosures

In the more general case of uneven absorption distribution, it is not normally possible to apply the specific techniques shown in the previous section. Instead, the mid-frequency reverberation time T_{mf} of a 10 x 9 x 8 metre enclosure is obtained using the SEA model for various absorption distributions. These results are then compared to the T_{mf} predictions made using other prediction methods, in order to establish the consistency of the SEA model in the non-homogeneous case. Here, T_{mf} was calculated using:

$$T_{mf} = \frac{T_{500} + T_{1k} + T_{2k}}{3} \quad (28)$$

where T_{500} is the T_{60} reverberation time in the 500 Hz octave band etc. The scattering coefficient was kept constant for each surface ($s = 0.08$); α_r was defined as 0.05 for an untreated wall and 0.8 for an absorbing wall. The results are shown in Table 2 overleaf.

Table 2: Predicted T_{mf} values (C – ceiling treatment, F – floor treatment, W3/W4 – treatment on side walls).

	Untreated	C	C, F	C, F, W3, W4	All
Sabine	4.22	1.32	0.80	0.44	0.30
Eyring	4.13	1.20	0.67	0.30	0.15
Millington-Sette	4.13	0.69	0.38	0.21	0.15
Fitzroy	4.13	2.75	2.99	1.49	0.15
Arau	4.13	1.77	1.30	0.41	0.15
Fitzroy-Kuttruff	4.58	1.11	0.54	0.28	0.15
EN 12354-6	5.37	2.42	1.84	1.02	0.74
SEA Model	4.17	1.85	1.53	1.42	0.16
CATT-Acoustic (T_{20})	4.16	1.83	1.59	0.79	0.17
CATT-Acoustic (T_{30})	4.15	1.89	1.56	0.80	0.17

It is suggested in Table 2 that the predictions made with the SEA model are generally consistent with the results obtained using the CATT-Acoustic model and the Arau prediction method. However, there is an exception for the case where the ceiling, floor, and side walls are acoustically treated; the prediction obtained using the SEA model is far longer than all other predictions except that of Fitzroy's equation, which tends to overestimate T_{60} .

This apparent discrepancy can be explained by examining the SEA decay curves illustrated in Figure 7.

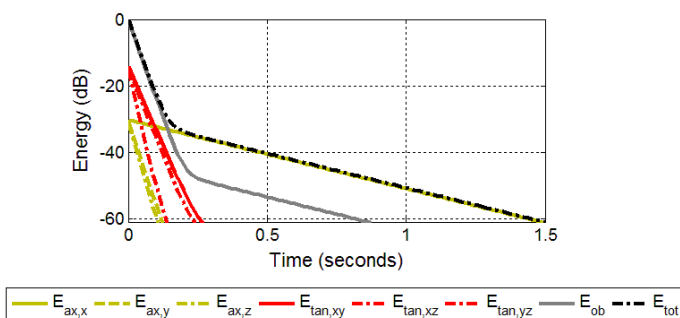


Figure 7: Energy decay curves of each subsystem in the SEA model, including the total energy decay curve.

Figure 7 shows that the start of the decay is dictated by the oblique mode group, which contains the most energy due to the large number of modes. At approximately -30 dB, an abrupt break point occurs, where the decay rate is determined by the x -direction axial mode group, and hence the decay curve becomes non-linear. This is because the x -direction axial mode group forms across the end walls, thereby circumventing the absorbing surfaces, which results in a relatively small decay rate and a long T_{60} prediction.

Due to the discrepancy, it is uncertain whether SEA predictions are valid for cases where absorbing material is placed on all surfaces except those that are normal to the longest room dimension; more experimental data is required to make this judgement. It may be possible that the effect of lateral damping is underestimated, which would explain the long predicted reverberation time.

Having said this, it should also be noted that the scattering coefficient is very small in this case. Increasing the scattering coefficient would have the effect of reducing the abruptness of the break point through increased coupling, which will reduce the T_{60} prediction.

In short, the SEA model has the potential for predicting the reverberation time in rooms with uneven absorption distributions, subject to further experimentation.

5 Conclusions

The SEA model presented by Nilsson was extended to accommodate arbitrary absorption distributions. A method of obtaining the damping and coupling loss factors from the absorption and scattering coefficients respectively was proposed. For homogeneous rooms, it was found that the results tended towards Eyring's formula, and the relative diffusivity of the room could be obtained from the gradient of the reverberation time curve. For non-homogeneous rooms, simulations showed that the SEA model generally gave consistent results, except for the case where absorption was placed on the ceiling, floor, and side walls.

Suggestions for future work include obtaining more experimental data for comparing with SEA predictions (one such comparison was conducted in [13] with varying degrees of success), as well as extending the SEA model further to include more complex scenarios, such as enclosures with non-homogeneous surfaces.

References

- [1] D. Fitzroy. 1959. The Journal of the Acoustical Society of America. *Reverberation Formula Which Seems to Be More Accurate with Nonuniform Distribution of Absorption*. **31**(7): p. 893-897.
- [2] Building Regulations, 2003. *Approved Document E: Resistance to the Passage of Sound*. London.
- [3] DES Building Bulletin 93. 2003. *Acoustic design of schools*. London: HMSO.
- [4] R. O. Neubauer. 2001. Building Acoustics. *Estimation of Reverberation Time in Rectangular Rooms with Non-Uniformly Distributed Absorption Using a Modified Fitzroy Equation*. **8**(2): p. 115-137.
- [5] H. Arau-Puchades. 1988. *Acustica. An improved reverberation formula*. **65**: p. 163-180.
- [6] British Engineering Standards International Organisation for Standardisation 12354-6. 2003. *Building Acoustics - Estimation of acoustic performance of buildings from the performance of elements - Part 6: Sound absorption in enclosed spaces* Standards Policy and Strategy Committee: London.
- [7] *CATT-Acoustic program v8.0*: Sweden.
- [8] *ODEON program v7.0*: Denmark.
- [9] E. Nilsson, 1992. Report TVBA-1004. *Decay Processes in Rooms with Non-Diffuse Sound Fields*. Faculty of Engineering, LTH. Lund University. Sweden.
- [10] R. H. Lyon and Richard G. DeJong, 1995. *Theory and application of statistical energy analysis*. 2nd ed., Boston; Oxford: Butterworth-Heinemann.
- [11] P. M. Morse and R. H. Bolt. 1944. Reviews of Modern Physics. *Sound Waves in Rooms*. **16**(3-4).
- [12] H. Kuttruff, 1991. *Room acoustics*. 3rd ed., London: Elsevier Applied Science.
- [13] L. I. Wilmshurst. 2011. MSc Thesis. *Predicting the Reverberation Time of Rooms with Uneven Absorption Distribution*. ISVR, University of Southampton.
- [14] C. F. Eyring. 1930. The Journal of the Acoustical Society of America. *Reverberation Time in "Dead" Rooms*. **1**(2A): p. 217-241.